Available online at www.sciencedirect.com
SCIENCE DIRECT®
International Journal of Heat and Mass Transfer 47 (2004) 4137–4152
International Journal of HEAT and MASS TRANSFER
www.elsevier.com/locate/ijhmt

Stabilization and elimination of transient unstable mixed convective vortex flow of air in a bottom heated horizontal flat duct by top plate heating

S.W. Chen, C.Y. Chang, J.T. Lir, T.F. Lin *

Department of Mechanical Engineering, National Chiao Tung University, Hsinchu, Taiwan 30010, R.O.C.

Received 30 March 2004; received in revised form 6 May 2004

Abstract

An experiment combining flow visualization and temperature measurement is carried out here to study the possible stabilization and elimination of the buoyancy driven unstable longitudinal, transverse and mixed vortex flow in mixed convection of air in a bottom heated horizontal flat duct by the top plate heating. The top plate temperature is varied systematically to examine its effects on the spatial and temporal flow structures in the duct. How the top plate temperature and the Reynolds and Rayleigh numbers of the flow affect the vortex flow characteristics is investigated in detail. Specifically the experiment is conducted for the Reynolds number varying from 1 to 50, Rayleigh number from 4000 to 8000 and the non-dimensional top plate temperature from 0 to 1 at an interval of 1/8, covering a wide range of the buoyancy-to-inertia ratio. The results indicate that the top plate heating substantially stabilizes and for some cases even eliminates the longitudinal, transverse, mixed longitudinal and transverse, and irregular vortex flows induced by the buoyancy associated with the heated bottom plate of the duct. At the high top plate temperature even the entire irregular vortex flow can be eliminated and the flow becomes unidirectional in the duct. Obviously the transient velocity and temperature oscillations in the flow are completely suppressed.
© 2004 Published by Elsevier Ltd.

1. Introduction

Vortex flow in the form of regular longitudinal and transverse rolls and a mixture of both induced at a slightly supercritical buoyancy in a mixed convective gas flow through a bottom heated and top cooled horizontal flat duct has been known for some time and is well documented in the literature. The buoyancy force acting on the gas flow results from the temperature difference between the hot bottom plate and the cold inlet gas entering the duct with the top plate being at the same temperature as the inlet gas. At a buoyancy well above the critical level unstable vortex flow appears, and the vortex rolls become deformed and time dependent. At an even higher buoyancy irregular rolls prevail in the duct. The highly efficient heat transfer associated with the unstable vortex flow is most welcome by the technological application such as cooling of microelectronic equipments [1] in which the efficient energy transport is of major concern. However, in the chemical vapor deposition (CVD) processes [2] used frequently to grow thin crystal films on silicon substrates, the presence of the vortex flow will result in a non-uniform chemical vapor deposition on the substrates, producing a thin crystal film of non-uniform thickness. Moreover, the unstable vortex flow will provoke a time-dependent deposition rate. Both the stable and unstable vortex flows are not welcome and should be avoided in the CVD processes. Simple means such as lowering the

* Corresponding author. Address: Department of Environmental Engineering, National Cheng Kung University, Tainan City 70101, Taiwan. Tel.: +886-6-236-4455; fax: +886-6-275-2790.
E-mail address: tflin@mail.ncku.edu.tw (T.F. Lin).

0017-9310/$ - see front matter © 2004 Published by Elsevier Ltd.
doi:10.1016/j.ijheatmasstransfer.2004.05.005

Nomenclature

A	aspect ratio, b/d
b, d, l	test section width, height, length
g	gravitational acceleration
Gr	Grashof number, $\beta g d^3(T_h - T_c)/\nu^2$
Gr/Re^2	buoyancy-to-inertia ratio
Pr	Prandtl number, ν/α
Ra	Rayleigh number, $\beta g d^3(T_h - T_c)/\alpha\nu$
Ra_{eff}	effective Rayleigh number
Re	Reynolds number, $W_m d/\nu$
t	time, s
T	temperature
T_c	temperature of the inlet air flow
T_h	temperature of the bottom plate
T_t	Temperature of the top plate
W_m	mean velocity components in z direction
x, y, z	dimensionless Cartesian coordinates all scaled with d
α	thermal diffusivity
β	thermal expansion coefficient
θ	dimensionless instantaneous air temperature, $(T - T_c)/(T_h - T_c)$
θ_b	dimensionless bottom plate temperature
θ_t	dimensionless top plate temperature, $(T_t - T_c)/(T_h - T_c)$
ε	effective buoyancy-to-inertia ratio, Ra_{eff}/Re^2
ν	kinematic viscosity

chamber pressure, which can effectively reduce the buoyancy effects [2], and accelerating the main gas flow through the substrate inclination have been adopted in real CVD processes to stabilize the vortex flow. But it is rather costly in reducing the chamber pressure. Besides, the substrate inclination is only good for stabilizing the temporal oscillations of the vortex flow [3]. It is not effective in wiping out the spatial structures of the vortex flow. Other methods need to be sought to stabilize the temporal flow oscillations and to suppress the formation of the spatial vortex structures in the mixed convective duct flow. In this study we explore the possibility of vortex flow stabilization and elimination by the top plate heating. Note that under this special arrangement of the thermal condition imposed on the duct, the flow streams near the bottom and top plates are, respectively, subjected to destabilizing and stabilizing temperature gradients. Particular attention is paid here to the investigation of how the stabilizing temperature gradient resulting from the top plate heating affects the vortex flow driven by the hot bottom plate. It should be pointed out that the use of the top plate heating to stabilize the buoyancy driven unstable vortex flow is similar to the hot wall CVD reactors [4]. But the details on how the hot wall stabilizes the flow in the reactor remain largely unexplored.

It is well known that the study of the buoyancy driven vortex flow in a horizontal flat duct reported in the literature mainly focuses on the situation in which the buoyancy is generated by the temperature difference between the hot bottom plate and the cold inlet flow with the top plate at the same cold temperature as the inlet flow. The effects of the top plate heating are less studied. The relevant literature on the present study is briefly reviewed in the following.

In a horizontal parallel plane channel with the bottom plate at a higher uniform temperature than the top one by ΔT, the critical Rayleigh number for the onset of the vortex flow was found to be around 1708 [5,6]. Ostrach and Kamotani [7,8] experimentally noted that longitudinal vortex rolls appeared at a supercritical temperature difference. Above the critical point, the heat transfer rate is increased by the thermal instability and the temperature field is strongly influenced by the motion of the vortex flow. When $Ra > 8000$, the vortex rolls become irregular. Hwang and Liu [9] visualized the onset of secondary flow and showed that the wave number of the vortex flow remained constant along the flow direction. Experiments conducted by Incropera et al. [10] and Maughan and Incropera [11] disclosed four flow regimes along the bottom plate-laminar forced convection, laminar mixed convection, transitional mixed convection, and turbulent free convection. The transition to turbulent flow was attributed to the breakdown of vortices due to the hydrodynamic instability. Besides, a correlation for the onset point was proposed. Criteria for the onset of vortex instability and the start of the transition from two-dimensional laminar flow to three-dimensional vortex flow in mixed convective air flow over an isothermally heated horizontal flat plate were established by Moharreri et al. [12]. The vortex flow regime starts with a stable laminar flow region where vortices develop and grow gradually and ends up with an unstable flow region where the vortices mix together and collapse to form a two-dimensional highly fluctuating turbulent flow regime.

In the mixed convection of the nitrogen gas between two horizontal, differentially heated parallel plates, Rosenberger and his colleagues [13,14] showed that at high Ra, the longitudinal rolls were unsteady and snaking. Besides, they identified the regime of Ra and Re leading to an unsteady flow. Nyce et al. [15] showed that the variations of velocity field in the axial and transverse directions were both consistent with the presence of both

longitudinal roll and transverse wave instabilities. The transverse rolls were noted at a very low Reynolds number by Ouazzani et al. [16,17]. They also refined the regime map to include the transverse rolls. The recent flow visualization from Yu et al. [18] showed that at a fixed *Ra* but in reducing *Re* the vortex flow transformed from the structure prevailed by the longitudinal rolls to transverse rolls in a sequence of stable longitudinal rolls, unstable longitudinal rolls, mixture of the longitudinal rolls and transverse rolls, and transverse rolls. Photographic results from Cheng and Shi [19] revealed the convective instability and chaotic phenomena driven by the buoyancy force. The effects of the thermophysical property variations on the vortex flow were recently examined by Wang et al. [20].

Some studies were reported in the literature concerning the effects of the top plate heating on the flow and heat transfer in the buoyancy driven mixed convection in a bottom heated horizontal flat duct. Osborne and Incropera [21] noted that with the top plate heated the heat transfer at the top plate was dominated by forced convection, while heat transfer at the bottom plate was characterized by mixed convection. Besides, the heat transfer enhancement associated with the vortex flow instability was restricted to the lower surface [22]. In fact, the Nusselt number at the top plate decreases slightly as the top plate temperature is raised. Later, the effects of the asymmetric top and bottom wall heating on the thermal instability were analyzed theoretically by Lee and Hwang [23]. They found that the top plate heating resulted in stable thermal stratification in the region near the top plate. These studies [21–23] implicitly suggested the suppression of the buoyancy driven flow and heat transfer by the top plate heating.

The above literature review clearly reveals that there has been a substantial amount of research carried out in the past on various aspects of the vortex flow and heat transfer solely driven by the bottom plate heating in mixed convection of gas in a horizontal flat duct. However, the vortex flows associated with other thermal boundary conditions are still poorly understood. Besides, very little is devoted to the development of means to stabilize the temporal vortex flow oscillation and to eliminate the spatial vortex flow structures. In the present study an experimental investigation will be conducted to explore the possible stabilization and elimination of the vortex flow of air in a bottom heated horizontal flat duct by the top plate heating. Systematic variation in the top plate temperature will be performed to examine its effects on the spatial and temporal flow structures in the mixed convection flow of air in a horizontal flat duct. How the top plate temperature, Reynolds and Rayleigh numbers of the flow affect the vortex flow characteristics will be investigated in detail.

2. Experimental apparatus and procedures

The experimental system established in the previous study [18] is also used here to investigate the effects of the top plate heating on the mixed convection of air in a bottom heated horizontal flat duct.

2.1. Experimental apparatus

The experimental apparatus is schematically shown in Fig. 1. The open-loop mixed convection apparatus consists of three parts: wind tunnel, test section, and measuring bench for the velocity and temperature, which is connected with a data acquisition unit.

The test section is a rectangular duct of 240 mm wide and 300 mm long with the duct height of 20 mm between the top and bottom walls, providing an aspect ratio of $A = 12$. The bottom plate of the test section is made of a 15 mm thick, high purity copper plate and is electrically heated by DC power supplies. The top plate of the test section is made of 3 mm thick glass plate and 2 mm thick plexiglass plate with a gap width of 3 mm. This top plate is reinforced by copper alloy frames to keep it flat. Distilled water is provided from a constant temperature circulation unit and flows into this gap to control the upper plate temperature.

The working fluid is air which is driven into the system by a 7.5 hp air compressor and sent into a 300-l high-pressure air tank. The air is first regulated by a pressure regulator and then passes through a settling chamber, a contraction nozzle, a developing section, the test section, and finally discharges into the ambient surrounding. The developing section is 1690 mm in length, approximately 84 times of the duct height. This insures the flow being fully developed at the inlet of the test section for $Re \leqslant 50$. An outlet section of 190 mm long is added to the test section to reduce the effects of the disturbances from discharging the flow to the ambient surrounding of the open-loop wind tunnel.

The volume flow rate of air is controlled and measured by two Hasting HFC flow controllers designed especially for low volume flow rates, with accuracy better than 1%. A thermocouple probe, which is an OMEGA (model HYP-O) mini hypodermic extremely small T-type thermocouple (33 gauge) implanted in a 1 in. long stainless steel hypodermic needle, supported by a three-way traversing stand is used to measure the instantaneous air temperature in the test section. In order to unravel the unsteady thermal characteristics of the vortex flow, the transient temperature oscillations are measured at selected detection points. The sampling rate of the data channel in the data acquisition system is set at 0.08 s per scan which is much shorter than the period of the flow oscillation in the low Reynolds number mixed convective flow considered here.

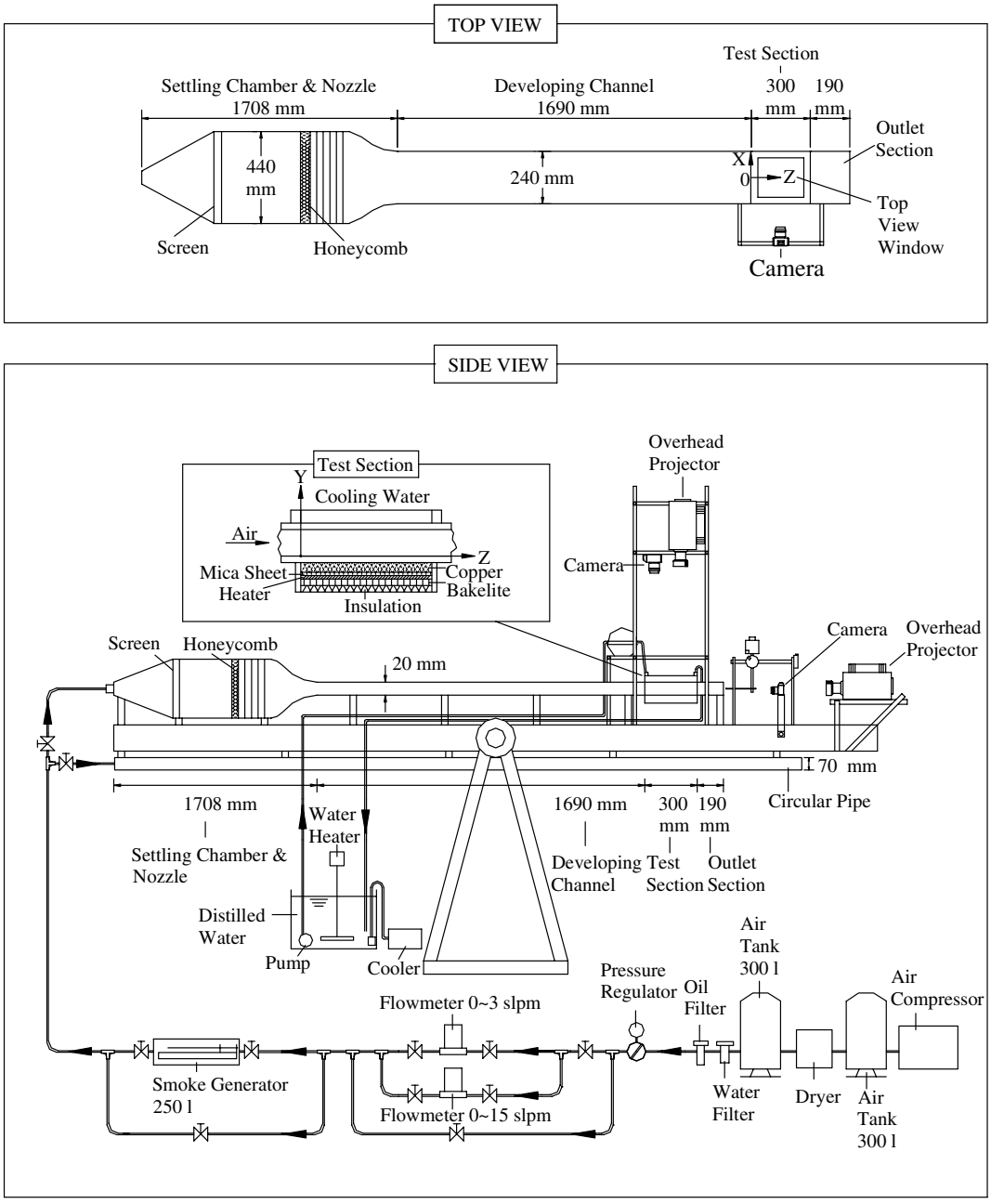

Fig. 1. Schematic of experimental apparatus and the chosen coordinate system for the test section.

Visualization of the buoyancy driven vortex flow in the test section is realized by injecting smoke tracers at some distance ahead of the settling chamber. By using a 1.5–2.5 mm plane light sheet from an overhead projector with an adjustable knife edge to illuminate the flow field containing these smoke particles, a sharp contrast could be achieved between the duct walls and smoke. Then the flow photos from the top, side and end views of the test section can be taken.

2.2. Experimental procedures

In each experiment the air compressor, dryer, DC power supplies, and the distilled water system are turned on first and set at the predetermined levels. Meanwhile, the distilled water is circulated over the top plate and all the experimental parameters are checked and recorded by the data acquisition unit. Usually, it takes about 3 h for the Rayleigh number and the distill water tempera-

ture to be raised to the test point, and another 2 h are needed to maintain the vortex flow at the stable or statistical state. Then we start the temperature measurement and flow visualization.

2.3. Analysis of data uncertainty

Uncertainties in the Rayleigh number, Reynolds number and other independent parameters are calculated according to the standard procedures established by Kline and McClintock [24]. The uncertainties of the thermophysical properties of air are included in the analysis. The fundamental thermophysical properties of the working fluid (air) are $\alpha = 0.220$ (cm^2/s), $\beta = 0.00335$ (1/K), $Pr = 0.737$ and $\nu = 0.162$ (cm^2/s) at 30 °C and 0.997 bar. The fluid properties are real time corrected based on the temperature and pressure detected at the inlet of the test section. In addition, the uncertainties of the control unsteadiness and temperature non-uniformity are accounted for in the evaluation of the data uncertainty. The analysis shows that the uncertainties of temperature, volume flow rate, dimensions, Reynolds number and Rayleigh number measurements are estimated to be ±0.15 °C, ±1%, ±0.005 mm, ±2% and ±5%, respectively.

3. Results and discussion

It is noted that the vortex flow considered here can be characterized by the three non-dimensional parameters—the Reynolds number Re, Rayleigh number Ra, and the dimensionless top plate temperature θ_t. They are defined as

$$Re = W_m d/\nu, \tag{1}$$

$$Ra = \beta g d^3 (T_h - T_c)/\alpha\nu \tag{2}$$

and

$$\theta_t = (T_t - T_c)/(T_h - T_c). \tag{3}$$

Selected results from the present flow visualization and temperature measurement will be presented here to illustrate the stabilization and elimination of the vortex flow in a bottom heated horizontal flat duct by the top plate heating. Particularly, we examine how the longitudinal, transverse, mixed, and irregular vortex flow patterns prevailed when the top plate is maintained at the same uniform temperature as the inlet air are influenced by various degrees of the top plate heating. In the experiments the Reynolds number of the flow is varied from 1.0 to 50.0 and Rayleigh number is fixed at 4000, 6000 and 8000. The top plate temperature is varied from T_c (the inlet air temperature) to T_h (the bottom plate temperature) at an interval of $(T_h - T_c)/8$. In terms of the dimensionless temperature defined as $\theta = (T - T_c)/(T_h - T_c)$, the inlet air and bottom plate are, respectively, at $\theta_i = 0$ and $\theta_b = 1$ and the top plate is at $\theta_t = 0.0$, 0.125, 0.25, 0.375, 0.5, 0.625, 0.725, 0.875 and 1.0.

3.1. Longitudinal vortex flow

The spatial structure of the longitudinal vortex flow affected by the top plate heating is manifested first by examining the top and end view flow photos at certain time instants at steady or statistical state for the cases with a high buoyancy-to-inertia ratio at $Re = 15.0$ and $Ra = 6003$ for various θ_t in Fig. 2. The changes of the roll number, size and onset location with various degrees of top plate heating are distinctly seen in the end view flow photos taken from the cross plane near the duct exit at $z = 12$. The stabilization and elimination of the unstable longitudinal vortex rolls by the top plate heating are more clearly shown in Fig. 3. Note that at $\theta_t = 0.0$ and 0.125 the flow is unsteady and four small, somewhat irregular rolls appear near the vertical central plane of the duct at $x = 0$ (Fig. 3(a) and (b)). The other longitudinal rolls are regular and steady. As θ_t is raised to 0.25, the four irregular rolls merge into two larger rolls (Fig. 3(c)). For θ_t raised further to 0.375 all the rolls in the duct are steady at long time when the initial flow transient dies out (Fig. 3(d)). At even higher θ_t of 0.5, 0.625 and 0.875 steady longitudinal rolls only appear in the regions near the duct sides (Fig. 3(e)–(g)) and the rolls in the duct core are eliminated. Besides, at higher top plate temperature the critical axial distance measuring from the duct inlet for the onset of the longitudinal rolls is somewhat longer when compared with that for $\theta_t = 0.0$. Finally at $\theta_t = 1.0$ all the vortex rolls are eliminated and the flow is unidirectional and hence forced convection dominated. The above results clearly show the highly effective stabilization and elimination of the unstable longitudinal vortex flow by the top plate heating.

3.2. Mixed longitudinal and transverse vortex flow

Next, we demonstrate how a regular mixed longitudinal and transverse vortex flow is influenced by the top plate heating. Note that in this mixed vortex flow for $\theta_t = 0$ the transverse rolls are repeatedly generated in the entry portion of the duct and then move downstream at a constant convection speed with the stationary longitudinal rolls induced in the side wall region. The details of this pattern for $\theta_t = 0$ were examined in our early study [18]. The present results show that raising the top plate temperature significantly weakens the moving transverse rolls in the duct core. In particular, at a higher θ_t the transverse rolls become shorter and are generated in the more downstream region. Meanwhile, more longitudinal rolls are induced. When θ_t exceeds a

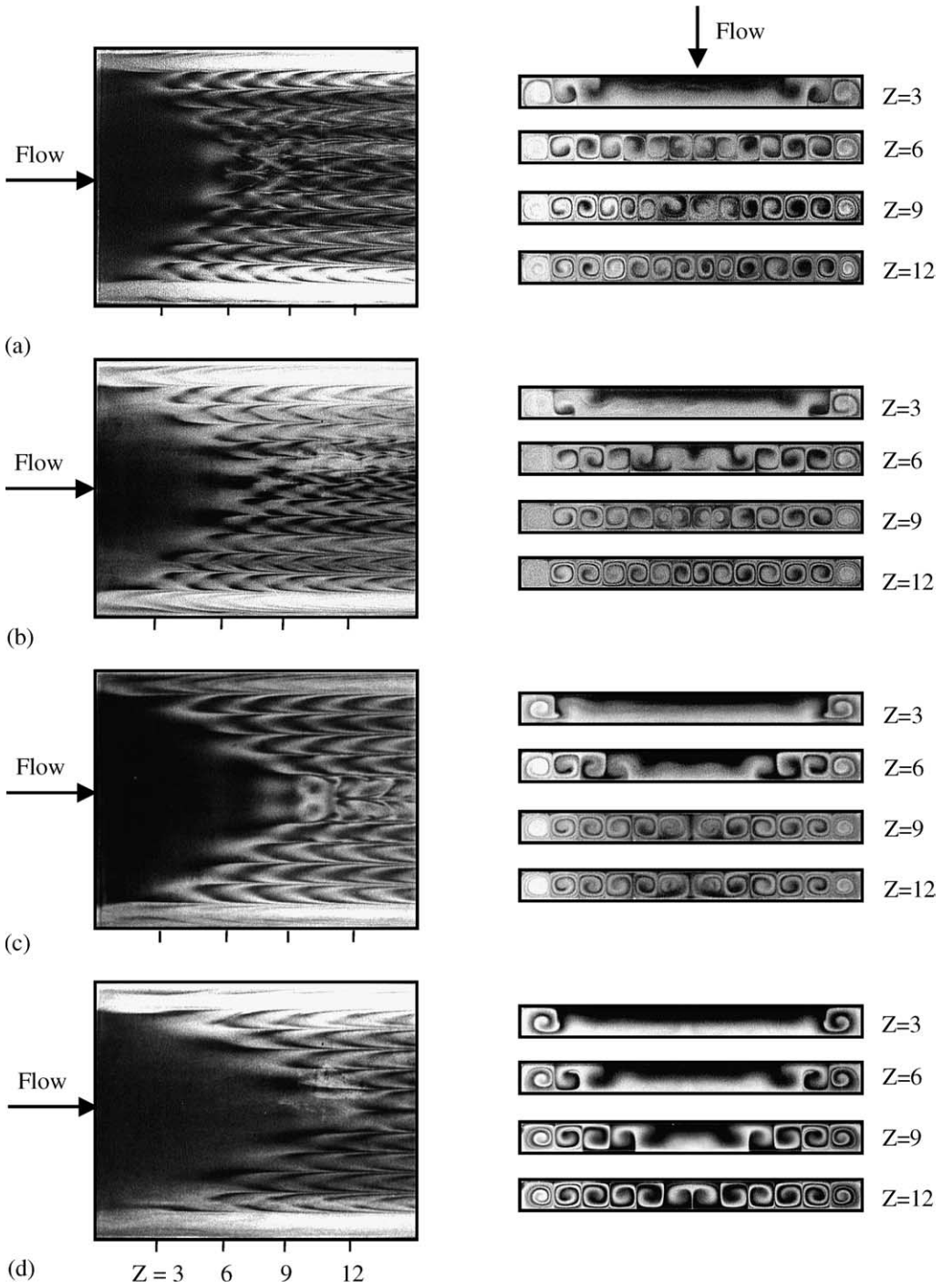

Fig. 2. Top and end view flow photos at steady or statistical state for $Ra = 6003$ and $Re = 15.0$ for various top plate temperatures at $\theta_t = 0.0$ (a), 0.125 (b), 0.25 (c), and 0.375 (d).

certain level, the transverse rolls all disappear and the entire duct is occupied by the longitudinal rolls. For θ_t raised further the longitudinal rolls in the duct core are gradually wiped out. Finally at $\theta_t = 1.0$, even the rolls near the duct sides are not induced and the flow is unidirectional.

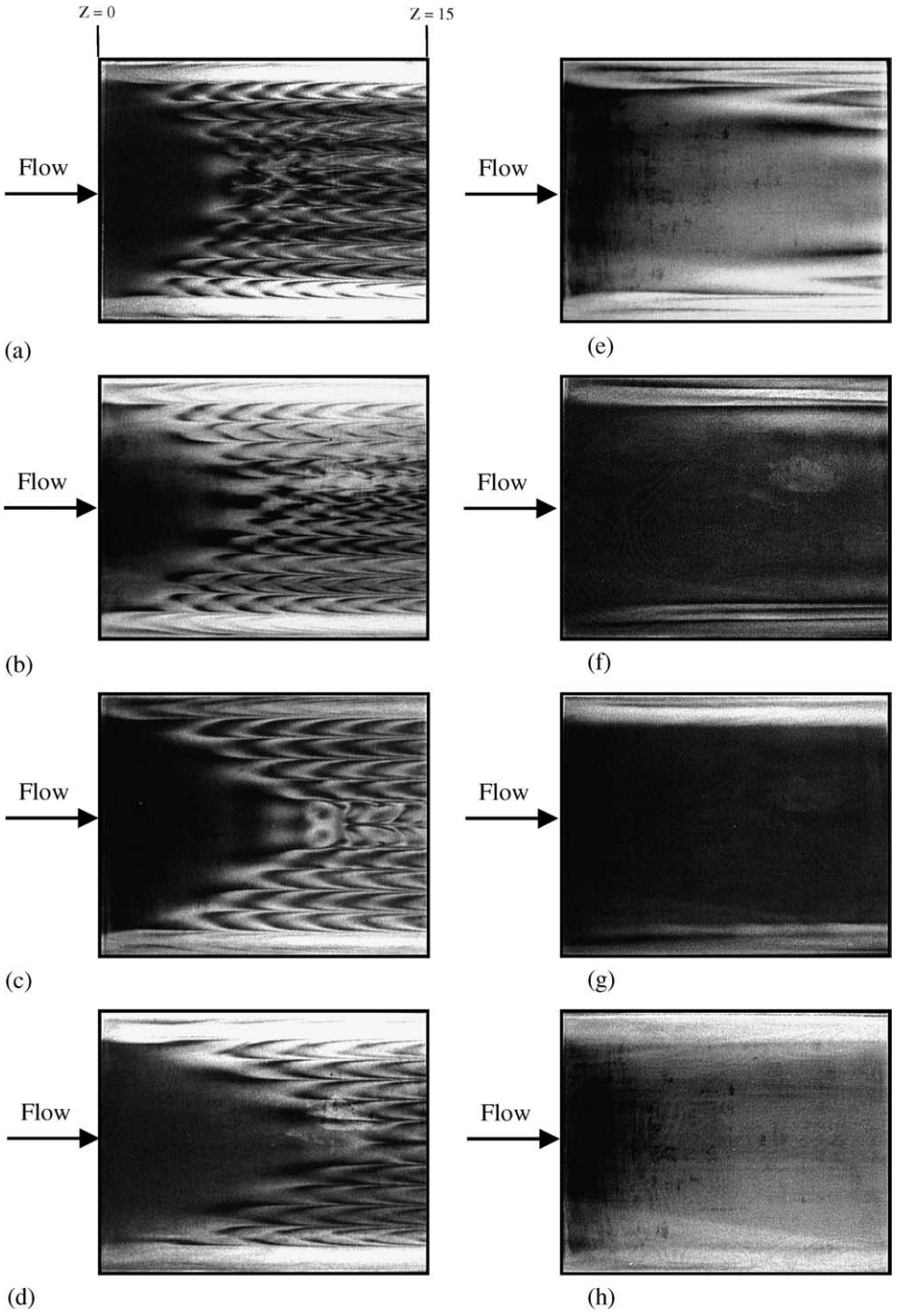

Fig. 3. Top view flow photos at steady or statistical state for $Ra = 6003$ and $Re = 15.0$ for various top plate temperatures at $\theta_t = 0.0$ (a), 0.125 (b), 0.25 (c), 0.375 (d), 0.5 (e), 0.625 (f), 0.875 (g), and 1.0 (h).

We move further to illustrate how an unsteady deformed mixed longitudinal and transverse vortex flow is stabilized by the top plate heating. This is shown in Fig. 4 for $Re = 5.0$ and $Ra = 6002$. At $\theta_t = 0.0$ both the longitudinal rolls near the side walls of the duct and the moving transverse rolls in the duct core are somewhat

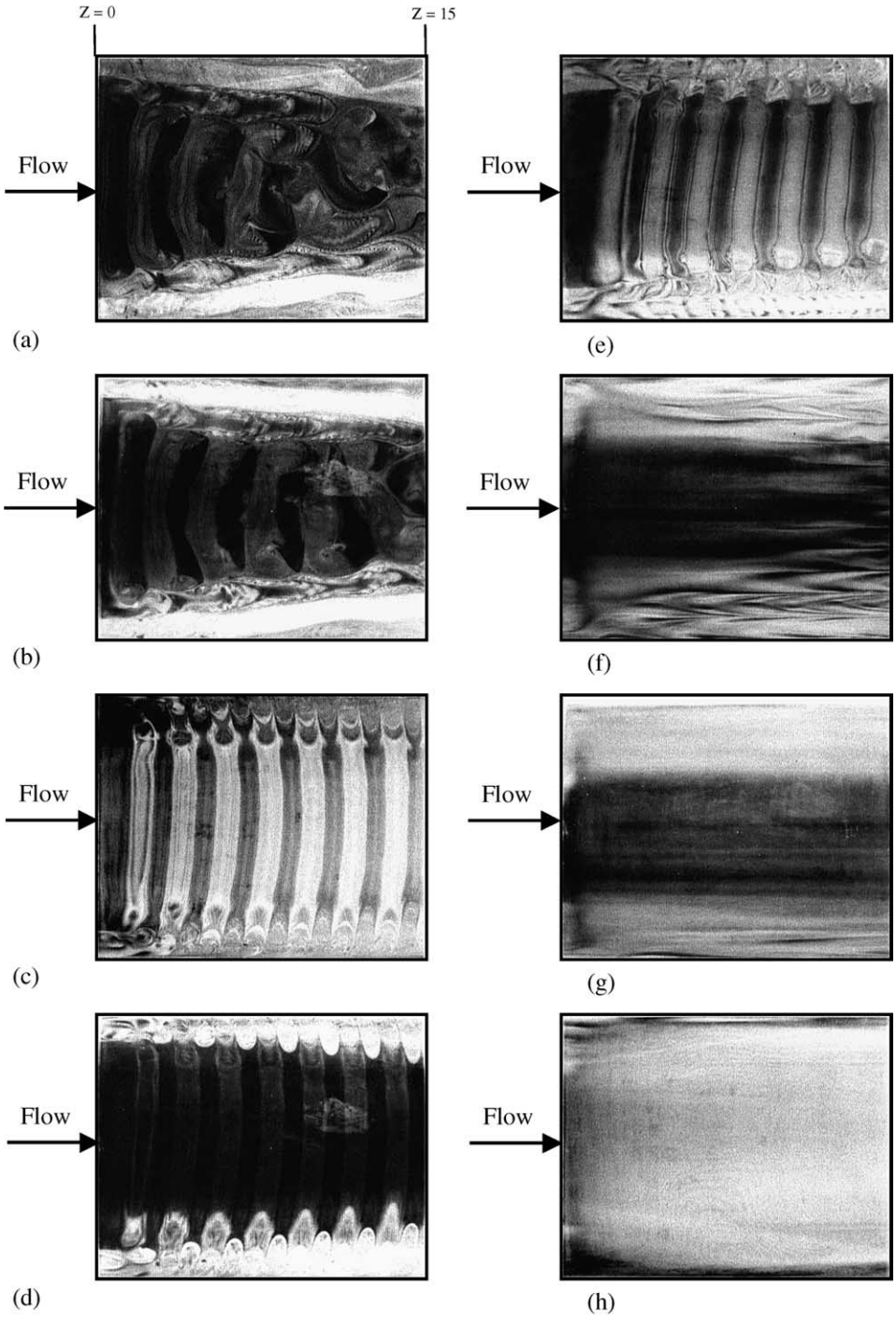

Fig. 4. Top view flow photos at steady or statistical state for $Ra = 6002$ and $Re = 5.0$ for various top plate temperatures at $\theta_t = 0.0$ (a), 0.125 (b), 0.25 (c), 0.375 (d), 0.5 (e), 0.625 (f), 0.875 (g), and 1.0 (h).

deformed (Fig. 4(a)). In fact, in the second half of the duct the rolls are highly irregular. It is of interest to note that for the slightly heated top plate with $\theta_t = 0.125$ the vortex flow is less irregular (Fig. 4(b)). As θ_t is raised to 0.25, all the irregular longitudinal rolls disappear and the duct is entirely filled with the regular moving

transverse rolls (Fig. 4(c)). Note that for further increases of θ_t to 0.375 and 0.5 some deformed longitudinal rolls appear again near the duct sides (Fig. 4(d) and (e)). At an even higher θ_t of 0.625 no transverse rolls are seen and the vortex flow in the duct is dominated by the steady longitudinal rolls (Fig. 4(f)). When θ_t is raised to a still higher level, less longitudinal rolls appear (Fig. 4(g)). Finally at $\theta_t = 1.0$, we have a unidirectional flow in the duct (Fig. 4(h)).

3.3. Transverse vortex flow

Then, the transverse vortex flow affected by the top plate heating is examined. We investigate the effects of the top plate heating on a strong and slightly irregular transverse vortex flow induced at an extremely high buoyancy-to-inertia ratio for $Re = 1.0$ and $Ra = 4003$. The results shown in Fig. 5 indicate that at $\theta_t = 0.0$ the entire duct is filled with slightly deformed transverse rolls and they move downstream at a very low speed at this low Reynolds number for $Re = 1.0$ (Fig. 5(a)). At the higher θ_t of 0.125, 0.25 and 0.375 the vortex flow patterns given in Fig. 5(b)–(d) are similar to that in Fig. 5(a) for $\theta_t = 0.0$. A close inspection of these results, however, reveals that at $\theta_t = 0.375$ the vortex rolls are smaller in size (Fig. 5(d)). Note that as θ_t is raised to 0.5 there is a big change in the vortex flow pattern (Fig. 5(e)). We now have two transverse rolls in the duct entry and twelve longitudinal rolls in the rest portion of the duct for $\theta_t = 0.5$. Besides, the transverse rolls are stationary and do not move downstream. Merging of the longitudinal and transverse rolls takes place in the upstream corner region. For θ_t raised to 0.625 and over all the vortex rolls are eliminated except the existence of one pair of longitudinal rolls in the side wall region of the duct and a stationary transverse roll in the duct entry (Fig. 5(f)–(h)).

3.4. Irregular vortex flow

Finally, it is of interest to investigate the possible stabilization and elimination of the irregular vortex flow driven at high buoyancy-to-inertia ratios by the top plate heating. This is illustrated in Fig. 6 for the cases with $Re = 5.0$ and $Ra = 8001$ at various top plate temperatures. The results show that at the low top plate temperature for $\theta_t \leqslant 0.25$ the flow is still dominated by the irregular vortex rolls (Fig. 6(a)–(c)). As θ_t is raised to 0.375 and 0.5 regular moving transverse rolls prevail in the duct (Fig. 6(d) and (e)). For the higher θ_t of 0.625 the duct is occupied by the mixed longitudinal and transverse rolls (Fig. 6(f)). For even higher θ_t of 0.75 and 1.0 only a few steady longitudinal rolls appear in the duct (Fig. 6(g) and (h)). The above results clearly demonstrate the significant flow stabilization produced by the top plate heating.

3.5. Transient temperature oscillations

To further reveal the detailed characteristics of the vortex flow affected by the top plate heating, selected data from the transient temperature measurement are presented in the following. Typical temperature data for the transverse vortex flow stabilized by the top plate heating for the cases with $Re = 5.0$ and $Ra = 4001$ are shown in Fig. 7. The results in Fig. 7 indicate that the amplitude and frequency of the temperature oscillations are only slightly influenced by the degree of the top plate heating as long as the flow remains dominated by the transverse rolls (Fig. 7(a)–(c)). But as θ_t is increased to 0.375, a big change in the vortex flow pattern occurs (Fig. 7(d)). We now have stable longitudinal rolls in the side wall region and unstable deformed longitudinal rolls in the duct core. The data in Fig. 7(d) clearly show that the temperature oscillations are somewhat irregular in the region dominated by the unstable rolls. Elsewhere the flow is steady.

Next, we examine the data in Fig. 8 for the deformed mixed vortex flow stabilized by the top plate heating for the cases with $Re = 5.0$ and $Ra = 6002$. The results indicate that the air temperature oscillates somewhat irregularly in time for the deformed mixed vortex flow at $\theta_t = 0.0$ (Fig. 8(a)). When the top plate is slightly heated at $\theta_t = 0.375$ the entire duct is filled with the transverse rolls and the temperature oscillates periodically in time at the same frequency and amplitude (Fig. 8(b)). For the higher θ_t of 0.5 a mixed vortex flow prevails (Fig. 8(c)). In the duct core dominated by the transverse rolls the temperature oscillation resembles that for $\theta_t = 0.375$ given in Fig. 8(b) except that near the duct inlet the amplitude of the temperature oscillation for $\theta_t = 0.5$ is substantially lower. While in the side wall region dominated by the longitudinal rolls the flow is steady and no temperature oscillation is detected. When θ_t is raised to 0.625 the longitudinal rolls become dominant and the temperature does not oscillate with time (Fig. 8(d)).

Finally, the temperature oscillations in the irregular vortex flow stabilized by the top plate heating are illustrated in Fig. 9. The results clearly show that the flow oscillates periodically in time in a much smaller amplitude for the higher θ_t of 0.375 and 0.5 at which the transverse vortex flow prevails (Fig. 9(c) and (d)). Again the temperature oscillation characteristics for $\theta_t = 0.375$ and 0.5 are nearly the same.

In summary, the present transient temperature data clearly manifest that the temporal flow oscillations in the transverse, mixed and even the highly irregular vortex flow can be significantly suppressed by the top plate heating. More specifically, as the vortex flow is changed by the top plate heating from that dominated by the irregular rolls to that prevailed by the transverse rolls,

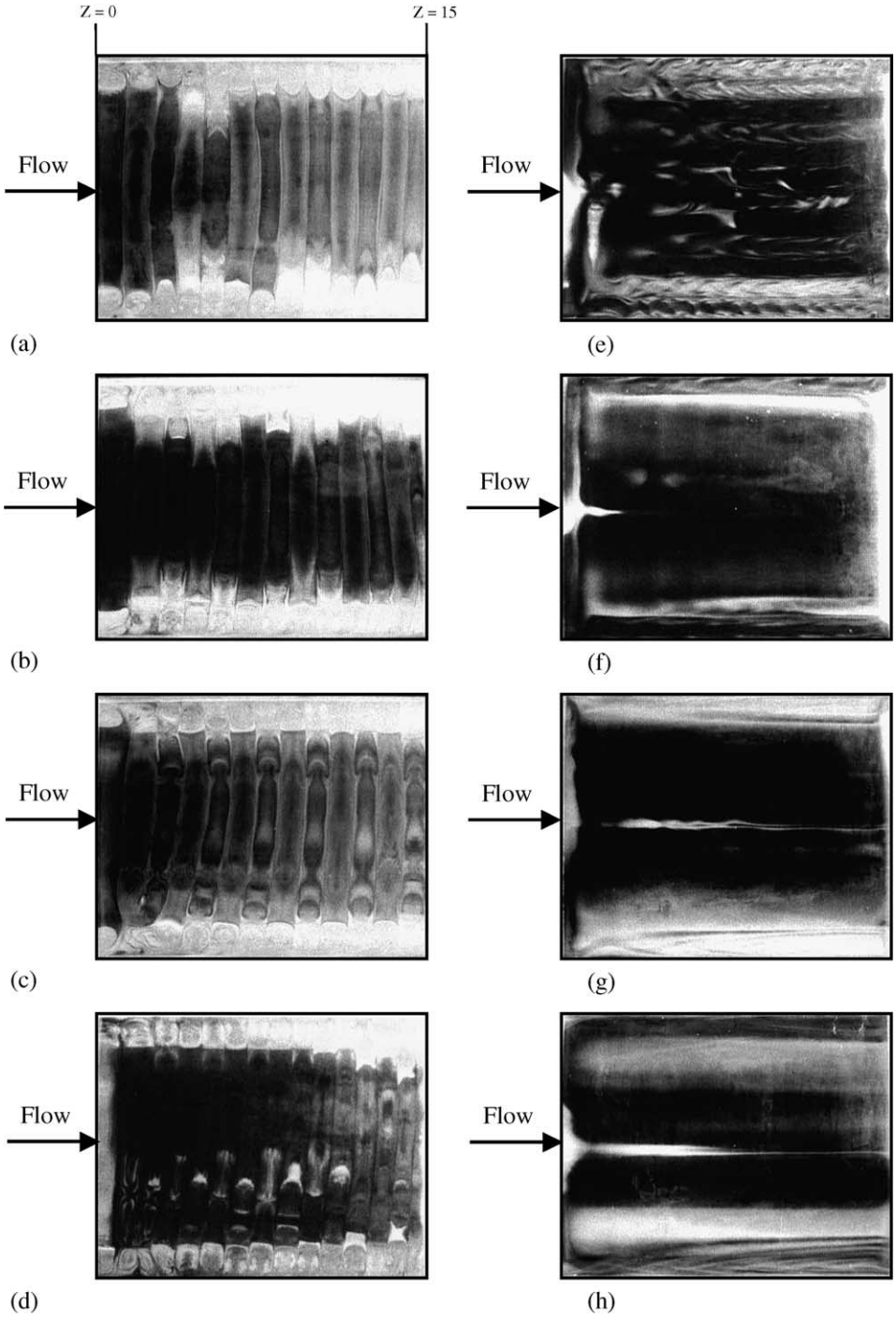

Fig. 5. Top view flow photos at steady or statistical state for $Ra = 4003$ and $Re = 1.0$ for various top plate temperatures at $\theta_t = 0.0$ (a), 0.125 (b), 0.25 (c), 0.375 (d), 0.5 (e), 0.625 (f), 0.75 (g), and 1.0 (h).

large amplitude irregular flow oscillations are greatly suppressed and the flow is in low amplitude time periodic oscillations. A further change of the transverse vortex flow to the longitudinal vortex flow completely suppresses the flow oscillation for the high top plate temperature.

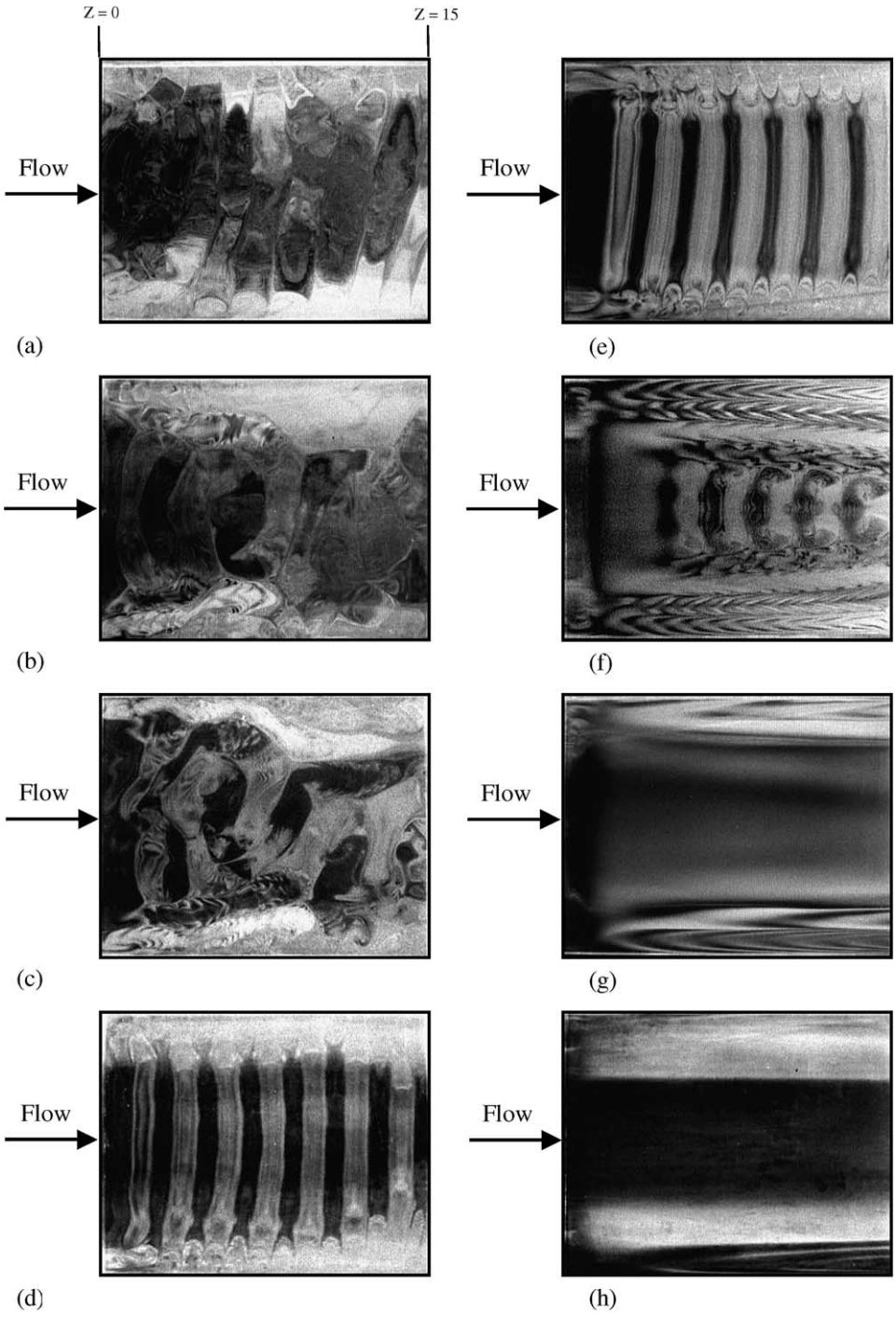

Fig. 6. Top view flow photos at steady or statistical state for $Ra = 8001$ and $Re = 5.0$ for various top plate temperatures at $\theta_t = 0.0$ (a), 0.125 (b), 0.25 (c), 0.375 (d), 0.5 (e), 0.625 (f), 0.75 (g), and 1.0 (h).

3.6. Effective Rayleigh number

The stabilization of the vortex flow by the top plate heating presented above can be more clearly characterized by defining an effective Rayleigh number, accounting for the differences in the inlet air temperature and the top and bottom plate temperatures. Based on all the vortex flow patterns obtained in the present study, we define

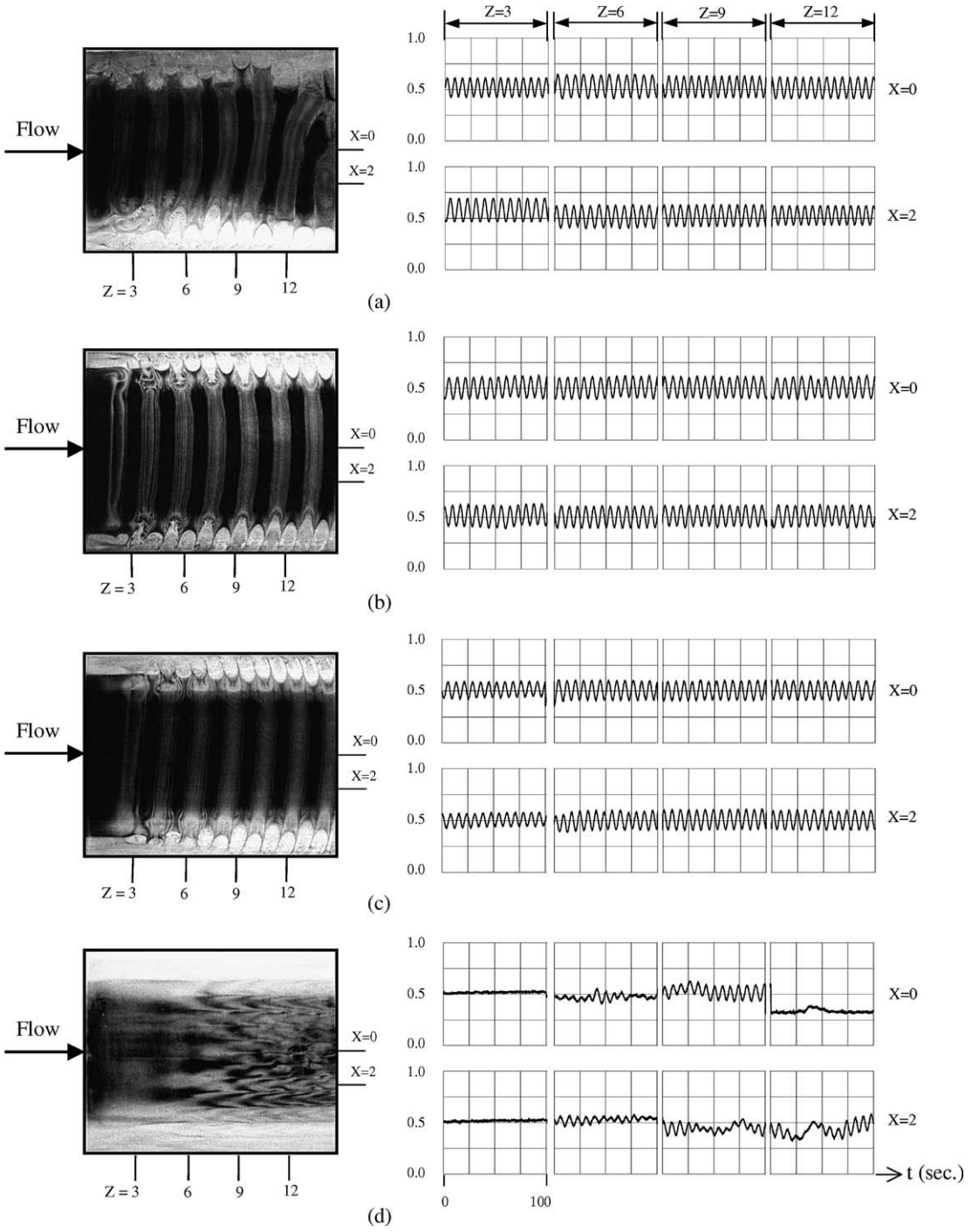

Fig. 7. Top view of vortex flow for $Ra = 4001$ and $Re = 5.0$ and the corresponding time records of air temperature at selected locations on the plane $y = 1/2$ for (a) $\theta_t = 0.0$, (b) $\theta_t = 0.125$, (c) $\theta_t = 0.25$, and (d) $\theta_t = 0.375$.

$$Ra_{\text{eff}} = Ra(1 - a\theta_t^b), \tag{4}$$

where $a = 0.9$ and $b = 0.75$. According to this effective Rayleigh number, the present data show that the unidirectional flow appears when the effective buoyancy-to-inertia ratio $\varepsilon(= Ra_{\text{eff}}/Re^2) < 58.7$ for $5 \leqslant Re \leqslant 20$. The longitudinal vortex flow dominates in the duct for ε ranging from 6.8 to 29.4 for Re in the range of 10–20.

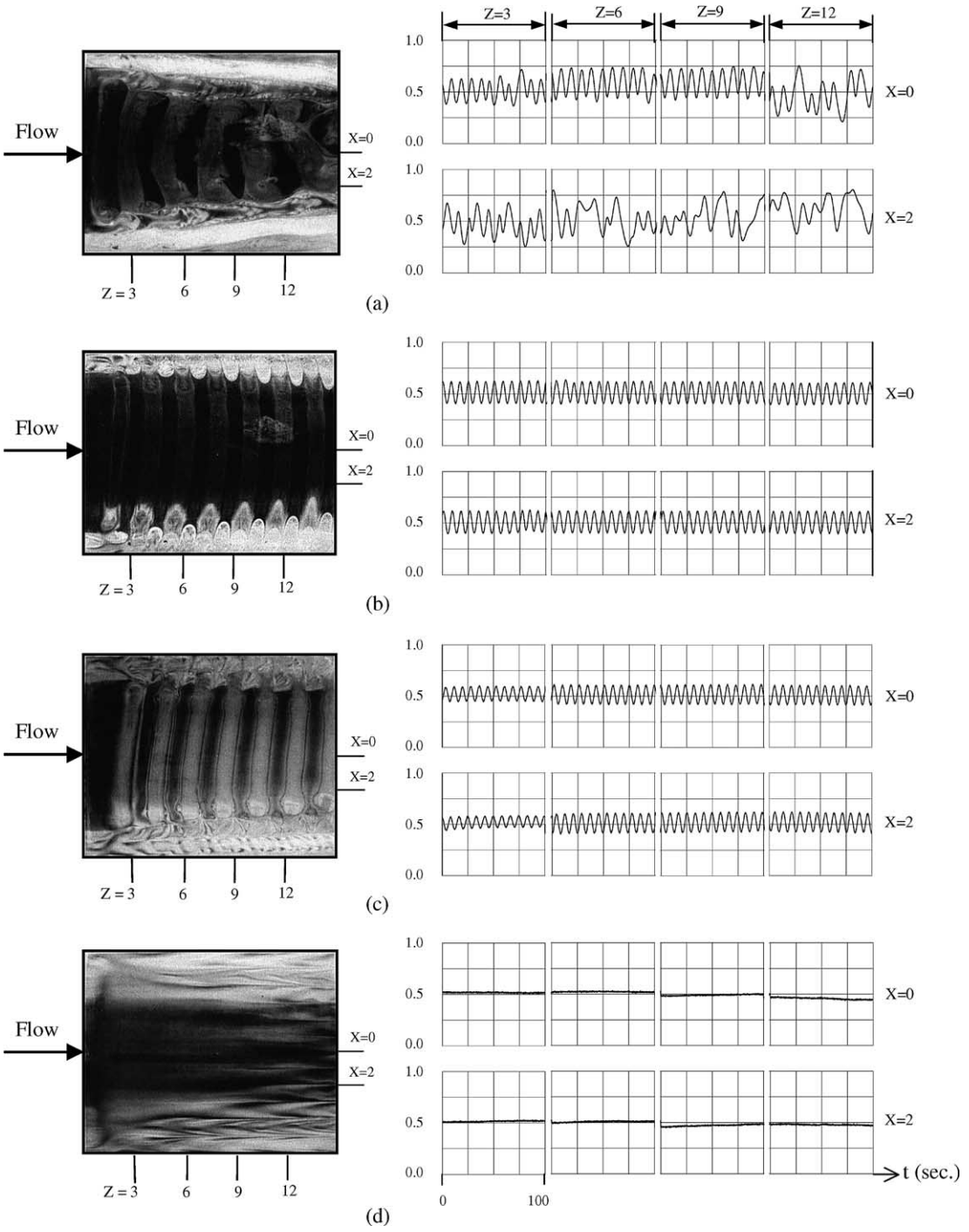

Fig. 8. Top view of vortex flow for $Ra = 6002$ and $Re = 5.0$ and the corresponding time records of air temperature at selected locations on the plane $y = 1/2$ for (a) $\theta_t = 0.125$, (b) $\theta_t = 0.375$, (c) $\theta_t = 0.5$, and (d) $\theta_t = 0.625$.

Note that for $20 < \varepsilon < 117.5$ and $5 < Re \leqslant 15$ the mixed vortex flow prevails in the duct. The transverse rolls are the dominant pattern when ε ranges from 109 to 2274 for $1 < Re \leqslant 5$.

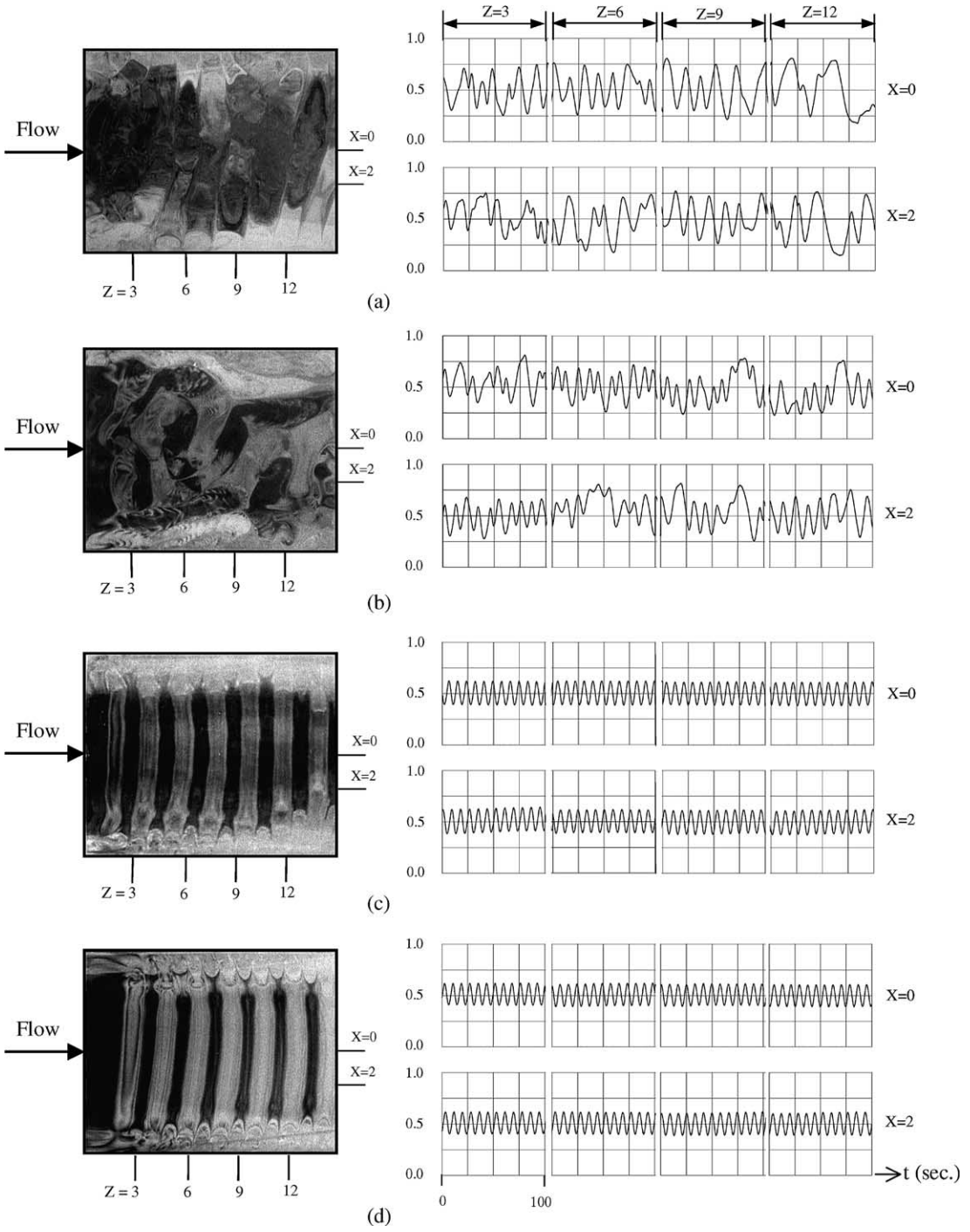

Fig. 9. Top view of vortex flow for $Ra = 8001$ and $Re = 5.0$, and the corresponding time records of air temperature at selected locations on the plane $y = 1/2$ for (a) $\theta_t = 0.0$, (b) $\theta_t = 0.25$, (c) $\theta_t = 0.375$, and (d) $\theta_t = 0.5$.

3.7. Concluding remarks

In the present study combined experimental flow visualization and temperature measurement have been carried out to unravel the effects of the top plate heating on the spatial and temporal structures of the mixed convective air flow through a bottom heated horizontal flat duct. In the experiments the Reynolds number of the

flow is varied from 1 to 50, Rayleigh number fixed at 8000, 6000, 4000, and the non-dimensional top plate temperature varied from 0 to 1. The major results obtained can be briefly summarized in the following.

(1) The top plate heating can produce highly effective stabilization and elimination of the longitudinal, transverse, mixed longitudinal and transverse, and irregular vortex flows. At the high top plate temperature all the vortex flow can be eliminated resulting in a unidirectional flow in the duct.
(2) At increasing top plate temperature the irregular vortex flow can be regularized to become time periodic and even become steady. Significant changes in the vortex flow patterns and temperature oscillations occur. But the oscillation frequency is only slightly affected as long as the transverse rolls still dominate in the duct.

During the course of this investigation, it has been realized that the buoyancy driven vortex flow in a horizontal flat duct heated from below can be significantly affected by the presence of a mounted block in the duct. Moreover, the gradual contraction of sidewalls in the duct so that the mean flow can be accelerated is expected to greatly affect the structures of the vortex flow. Some flow stabilization may be obtained. These will be explored in the near future.

Acknowledgements

The financial support of this study by the engineering division of National Science Council of Taiwan, ROC through the NSC83 0404 E009 054 is greatly appreciated.

References

[1] F.P. Incropera, Convective heat transfer in electronic equipment cooling, ASME. J. Heat Transfer 110 (1988) 1097–1111.
[2] M.L. Hitchman, K.F. Jensen, Chemical Vapor Deposition (Principle and Application), 1993, pp. 245–381 (Chapter 6).
[3] W.S. Tseng, W.L. Lin, C.P. Yin, C.L. Lin, T.F. Lin, Stabilization of buoyancy driven unstable vortex flow in mixed convection of air in a rectangular duct by tapering its top plate, ASME. J. Heat Transfer 122 (2000) 58–65.
[4] C. Galewski, W.G. Oldham, Modeling of a high throughput hot-wall reactor for selective epitaxial growth of silicon, IEEE Trans. Semicond. Manufact. 5 (1992) 169–179.
[5] Y. Mori, Y. Uchida, Forced convective heat transfer between horizontal flat plates, Int. J. Heat Mass Transfer 9 (1966) 803–817.
[6] M. Akiyama, G.J. Hwang, K.C. Cheng, Experiments on the onset of longitudinal vortices in laminar forced convection between horizontal plates, ASME. J. Heat Transfer 93 (1971) 335–341.
[7] S. Ostrach, Y. Kamotani, Heat transfer augmentation in laminar fully developed channel flow by means of heating from below, ASME. J. Heat Transfer 97 (1975) 220–225.
[8] Y. Kamotani, S. Ostrach, Effect of thermal instability on thermally developing laminar channel flow, ASME. J. Heat Transfer 98 (1976) 62–66.
[9] G.J. Hwang, C.L. Liu, An experimental study of convective instability in the thermal entrance region of a horizontal parallel-plate channel heated from below, Can. J. Chem. Eng. 54 (1976) 521–525.
[10] F.P. Incropera, A.L. Knox, J.R. Maughan, Mixed-convection flow and heat transfer in the entrance region of a horizontal rectangular duct, ASME. J. Heat Transfer 109 (1987) 434–439.
[11] J.R. Maughan, F.P. Incropera, Regions of heat transfer enhancement for laminar mixed convection in a parallel plate channel, Int. J. Heat Mass Transfer 33 (1990) 555–570.
[12] S.S. Moharreri, B.F. Armaly, T.S. Chen, Measurements in the transition vortex flow regime of mixed convection above a horizontal heated plate, ASME. J. Heat Transfer 110 (1988) 358–365.
[13] K.C. Chiu, F. Rosenberger, Mixed convection between horizontal plate-I. Entrance effects, Int. J. Heat Mass Transfer 30 (1987) 1645–1654.
[14] K.C. Chiu, J. Ouazzani, F. Rosenberger, Mixed convection between horizontal plate-Π. Fully developed flow, Int. J. Heat Mass Transfer 30 (1987) 1655–1662.
[15] T.A. Nyce, J. Ouazzani, A. Durand-Daubin, F. Rosenberger, Mixed convection in a horizontal rectangular channel—experimental and numerical velocity distributions, Int. J. Heat Mass Transfer 35 (1992) 1481–1494.
[16] M.T. Ouazzani, J.P. Caltagirone, G. Meyer, A. Mojtabi, Etude numérique et expérimentale de la convection mixte entre deux plans horizontaux à températures différences, Int. J. Heat Mass Transfer 32 (1989) 261–269.
[17] M.T. Ouazzani, J.K. Platten, A. Mojtabi, Etude expérimentale de la convection mixte entre deux plans horizontaux à températures différences-II, Int. J. Heat Mass Transfer 33 (1990) 1417–1427.
[18] C.H. Yu, M.Y. Chang, T.F. Lin, Structures of moving transverse and mixed rolls in mixed convection in a horizontal plane channel, Int. J. Heat Mass Transfer 40 (1996) 333–346.
[19] K.C. Cheng, L. Shi, Visualization of convective instability phenomena in entrance region of a horizontal rectangular channel heated from below and/or cooled from above, Exp. Heat Transfer 7 (1994) 235–248.
[20] Q. Wang, H. Yoo, Y. Jaluria, Convection in a horizontal rectangular duct under constant and variable property formulations, Int. J. Heat Mass Transfer 46 (2003) 297–310.
[21] D.G. Osborne, F.P. Incropera, Laminar, mixed convection heat transfer for flow between horizontal parallel plates with asymmetric heating, Int. J. Heat Mass Transfer 28 (1985) 207–217.

[22] J.R. Maughan, F.P. Incropera, Fully developed mixed convection in a horizontal channel heated uniformly from above and below, Numer. Heat Transfer A 17 (1990) 417–430.
[23] F.S. Lee, G.J. Hwang, The effect of asymmetric heating on the onset of thermal instability in the thermal entrance region of a parallel plate channel, Int. J. Heat Mass Transfer 34 (1991) 2207–2218.
[24] S.J. Kline, F.A. McClintock, Describing uncertainties in single-sample experiments, Mech. Eng. 75 (1953) 3–12.